# Microstructure-dependent viscosity in concentrated suspensions of soft spheres

S. E. Paulin and Bruce J. Ackerson[*]

*Department of Physics, Oklahoma State University, Stillwater, Oklahoma 74078*

M. S. Wolfe

*E. I. du Pont de Nemours and Company, Wilmington, Delaware 19880*

Monodisperse colloidal suspensions of polymethylmethacrylate spheres swollen in benzyl alcohol have been rheologically examined under applied steady and oscillatory shear while simultaneously monitoring microstructure via light scattering. In concentrated samples, long-lived nonequilibrium microstructures can be induced, corresponding to random hexagonal-close-packed planes (hcp) stacked in the direction of the shear gradient. The direction of closest packing within each hcp plane can be oriented along either the vorticity or direction of flow. Creep and creep recovery measurements have been examined for each of these two orientations as a function of particle concentration and stress. Results indicate a strain-dependent dissipative process correlated with changes sample microstructure, while dynamic measurements of the storage modulus show no significant difference between microstructures. We argue that instantaneous viscosities can be measured and show how they are correlated with changes in particle microstructure. The observed elastic response in these suspensions will be shown to be due to local microstructure and particle deformation. [S1063-651X(97)16105-0]

PACS number(s): 82.70.−y, 83.85.Jn, 78.20.Ci

## I. INTRODUCTION

The viscoelastic behavior observed in complex fluids may be broadly characterized as due to the effects of fading memory, where the present rheological response of the material is dependent upon its past deformation history. The strength of this dependence is dictated by a number of factors, but may be gauged by the Deborah number De [1]. This dimensionless quantity is defined as the ratio of some intrinsic relaxation time associated with the material's approach to steady state under applied deformation, to that of an observation time. The observation time may be the duration of the experiment. In colloidal suspensions, the relaxation process may be due to either a dissipation of stored elastic energy or a slow but purely dissipative reorganization of particles while subjected to flow. Memory effects therefore become important when De $\geq$ 1, and in some cases are observed as thixotropic behavior. Charge-stabilized, electrorheological, and flocculated dispersions typically exhibit this type of behavior. Under applied stress, the breakage and reformation of interparticle bonds responsible for the suspensions structure, approaches steady state on a time scale dependent upon thermodynamic and interparticle contributions to the bulk stress. This behavior is reversible in the sense that the suspension structure rebuilds itself once the stress is removed.

Unlike electrorheological or flocculated dispersions, the role of equilibrium structure in a moderately concentrated colloidal fluid of hard spheres is less obvious. Here, viscoelastic behavior has been identified as due to configurational free energy contained in the suspensions equilibrium microstructure [3]. Due to hydrodynamic interactions between the particles and surrounding fluid, shear thinning results from a perturbation of this microstructure from equilibrium. The change in particle configuration is assumed to be instantaneous with respect to a change in the applied shear stress, rendering the suspensions memory negligible (De $\ll$ 1) and the suspension a generalized Newtonian fluid [2]. Between thixotropic and generalized Newtonian behavior, there is a wide variety of viscoelastic phenomena which can be observed. Some of the most interesting of this behavior can be found in highly concentrated (glassy) suspensions of hard or nearly hard spheres, due to their ability to shear order into long-lived structures [4–8].

Highly concentrated suspensions are unique in that the times required for thermodynamic relaxation to equilibrium may be prohibitively long. This behavior may not be reversible, unlike thixotropic or generalized Newtonian materials, and may posses no yield stress. If such a system is prepared in a metastable state, geometrical constraints such as those imposed by certain shear ordered microstructures, will contribute to the rheological behavior in a measurable way. In this paper we will examine, via light scattering and rheological measurements, shear-induced microstructures in concentrated dispersions of polymethylmethacrylate (PMMA) spheres swollen in benzyl alcohol. These suspensions have been found to behave as soft spheres with a repulsive $1/r^{20}$ interparticle potential, and to exhibit equilibrium and shear-induced nonequilibrium phases similar to those found in sterically stabilized suspension of PMMA ''hard spheres'' [4–6,9–11]. In the glassy phase, the microgel suspensions are capable of maintaining a metastable, shear oriented state upon cessation of flow. As determined by light scattering, these nonequilibrium microstructures consist of ordered layers of hexagonal-close-packed (hcp) planes, randomly stacked parallel to the the direction of the shear gradient in simple shear. The closest-packed direction can be oriented either parallel to the velocity or vorticity direction, depend-

---

*Author to whom correspondence should be addressed.

ing upon the initial preparation. A description of these initial microstates relative to the stacking of hexagonal-close-packed planes of particles will be addressed in Sec. II.

We will show that the creep response associated with a given shear-induced structure, which differs in its closest-packed direction relative to the direction of flow, is the result of a viscous, strain-dependent reordering of the microstructure. Here, the viscous response of these given states can be measured as an instantaneous viscosity and correlated with their microstructural evolution. The relaxation of elastically stored energy in these microgels is found to be complete within less than 2 s, and presumed due to local particle deformation. The linear dynamic rheological response of these microstructures have been found to be similar, and results of these measurements will also be presented.

## II. EXPERIMENTAL DETAILS AND RESULTS

The particles, referred to as PMMA microgels, were prepared by emulsion polymerization of methyl methacrylate with 10% tetraethylene glycol dimethacrylate as the crosslinker, and have been discussed previously [12]. When dispersed in benzyl alcohol, particle swelling occurs. Their nonswollen radius is 150 nm, swelling to 324 nm when dispersed [6]. For the swollen particles, an effective volume fraction may be defined as $\phi^* = [\eta]C/2.5$. This is obtained by comparing Einstein's dilute limit expression for the reduced viscosity of a suspension of hard spheres with its power series expression in concentration, $C$. Here, $[\eta]$ is the intrinsic viscosity measured for the suspensions in the limit of vanishing $C$, and has been found to be $[\eta] = 36$ ml/g, via capillary viscometry measurements. Although particle deswelling and deformation will lead to effective volume fractions in excess of 0.749, the maximum packing fraction for hard spheres, the effective volume fraction obtained from the above definition has been shown to be a useful scaled variable in characterizing the suspension viscoelastic, equilibrium, and nonequilibrium phase behavior [6,12].

Rheo-optical studies were performed utilizing a Bohlin Instruments constant stress rheometer. Equipped with a glass C14 concentric cylinder shear cell, the rheometer was used to measure the creep and recovery compliance and dynamic moduli, while simultaneously monitoring suspension microstructure. The radius of the rotating inner bob is 7 mm, with a gap size of 0.7 mm between the bob and fixed outer cup. The temperature of the shear cell was not controlled and left to the ambient value ($\sim 20 \pm 2$ °C). To prevent solvent evaporation, a solvent trap consisting of a knife edge and trough filled with benzyl alcohol was utilized. The low volatility of benzyl alcohol, coupled with the solvent trap, allowed measurements to be made over a period of days with no appreciable evaporation. Viscosity as a function of applied shear stress was periodically measured to monitor any volume fraction changes due to solvent evaporation.

The scattering geometry of the rheo-optical couette is shown in Fig. 1. Here a helium cadmium laser ($\lambda = 442$ nm) probed the suspension microstructure approximately in the velocity-vorticity plane, the magnitude of the scattering vector being defined as $|\mathbf{k}| = |\mathbf{k}_i - \mathbf{k}_s| = (4\pi n/\lambda)\sin\theta/2$. Here, $\mathbf{k}_i$ and $\mathbf{k}_s$ are the incident and scattered wave vectors, respectively, $n$ is the solvent refractive
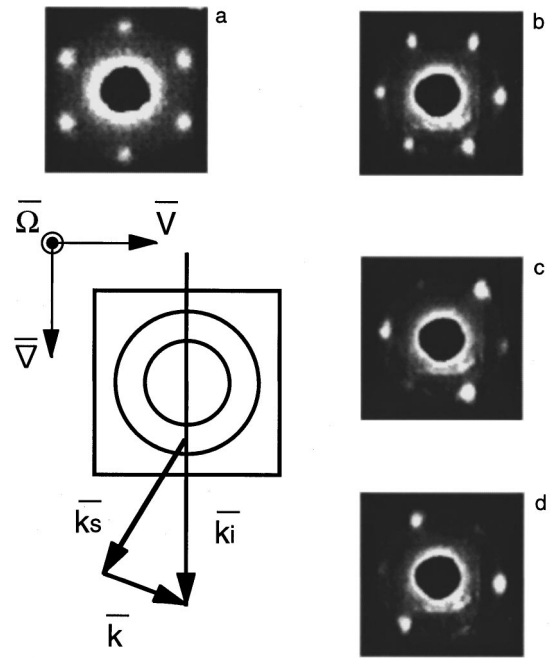


FIG. 1. Scattering images from structures identified as random stacked hexagonal-close-packed planes with the closest-packed direction oriented parallel to (a) the velocity direction (presheared structure), and (b) the vorticity direction (pre-fcc structure). (c) and (d) are typical face-centered-cubic twin structures. The dark center in the scattering patterns is a beam stop. The schematic cell diagram presents a top view where the sample is contained between the two circles representing the outer stationary couette wall and the inner rotating wall. The square represents the index matching bath with the bottom wall in this figure, being the position where the accompanying scattering patterns are projected. The $k$-space unit vectors apply to the region in the sample where the scattered vector $\mathbf{k}_s$ originates.

index, $\theta$ is the scattering angle, and $\lambda$ is the radiation wavelength. To reduce the effects of refraction, the couette was immersed in a rectangular index matching bath of glycerine, and the scattering imaged directly on the front of the index bath container. The observed scattering patterns were video taped for digitizing and analysis.

The rheo-optical measurements made in this work specifically examine the rheological consequences of different shear-induced microstructures. These microstructures are distinct, as can be seen from the light diffraction scattering patterns shown in Figs. 1(a) and 1(b). Similar scattering patterns to these have previously been observed in charged and sterically stabilized suspensions of colloidal spheres subjected to shear flow [4,13]. Sample preparation consisted of shearing the suspension at a rate of approximately 66 s$^{-1}$ for 300 s, followed by 180 s of quiescence. This shearing orients the microstructure to produce the observed scattering shown in Fig. 1(a). This structure was the initial state of the sample for measurements denoted as presheared. Preparation of the microstructure associated with Fig. 1(b) was the same as the presheared, except the bob was moved vertically up and down after the initial shearing. This microstructural orientation is termed pre-fcc. Such a name is chosen as the pre-fcc structure evolves under strain into one of the twins associated with a fcc crystal [see Figs. 1(c) and 1(d)], as will be

made clear in the discussion. The number of vertical repetitions varied from 25 to 100 depending upon the sample volume fraction, with the larger number being required for higher concentrations. The time and rate of preshearing, quiescence time, and number and amplitude ($\sim$strain of one) of vertical repetitions, were all determined by experience with the microgels as reasonable parameters which brought the sample back to some uniform initial state. Reproducibility of the observed scattering was reasonable, although no consistent and quantitative measurements of spot intensity or width were made during this set of experiments. Concentration of the samples examined was sufficiently large that these microstructures remained for an indefinite period of time once induced, thus allowing them to be rheologically probed. However, in some samples a brightening and narrowing of the observed intensity maxima in the scattering patterns occured over a period of hours, perhaps due to the annealing of local defects. Therefore, to ensure consistency, measurements were made on structures within approximately five minutes after induction.

In our creep measurements a constant stress is applied to the inner bob of the couette cell and the resulting motion of the bob is quantified in terms creep, the measured strain divided by the applied stress. Creep depends on both the viscous and elastic properties of the medium. In the recovery portion of a creep measurement, the stress on the inner bob is eliminated and creep recovery to the original unstressed state is monitored. Energy stored in elastic deformation will result in creep recovery. Energy lost to viscous heating will show no recovery. In general, there is only partial recovery due to viscous losses or slip.

Stress dependent creep, $J_\sigma(t)$, and creep recovery, $J_{r,\sigma}(t_c, t)$, measurements were made on the two microstructures at effective volume fractions of $\phi^* = 1.22$, $1.03$, $0.783$, and $0.681$, over a series of discrete times ranging from $t = 2$ s to $2.2 \times 10^4$ s. Here the subscripts on the compliance functions are to denote that they are stress, $\sigma$, dependent. Measurements were repeated over a range of applied stresses for each effective volume fraction. Typical stress-dependent creep behavior for these two structures are shown in Figs. 2(a) and 2(b), for $\phi^* = 1.03$ at $\sigma = 5$ and 8 Pa, respectively. The initial oscillation at short times appears in nearly all measurements. We do not observe these oscillations during creep recovery. It is believed that this oscillation is due to the controlling circuitry of the rheometer. The distinct form for each creep function at increased times is peculiar to the initial microstructural state and applied stress. The open circles in each graph correspond to the starting microstructure shown in Fig. 1(a), and the solid circles that of Fig. 1(b).

Creep measurements typically exhibit both elastic and dissipative relaxation processes. Therefore, recovery measurements were made as a function of creep time in order to decouple the elastic and dissipative memory effects in the microgels. The total recoverable strain measured for several applied stresses and over a series of different applied times, $t_c$, is shown in Fig. 3. Here, the suspension was prepared in either the presheared or pre-fcc state, as indicated by the open and filled symbols, respectively. The total recoverable strain is found to be nearly constant over all time scales measured, and independent of the microstructure. This result indicates that the suspension is elastically relaxed within
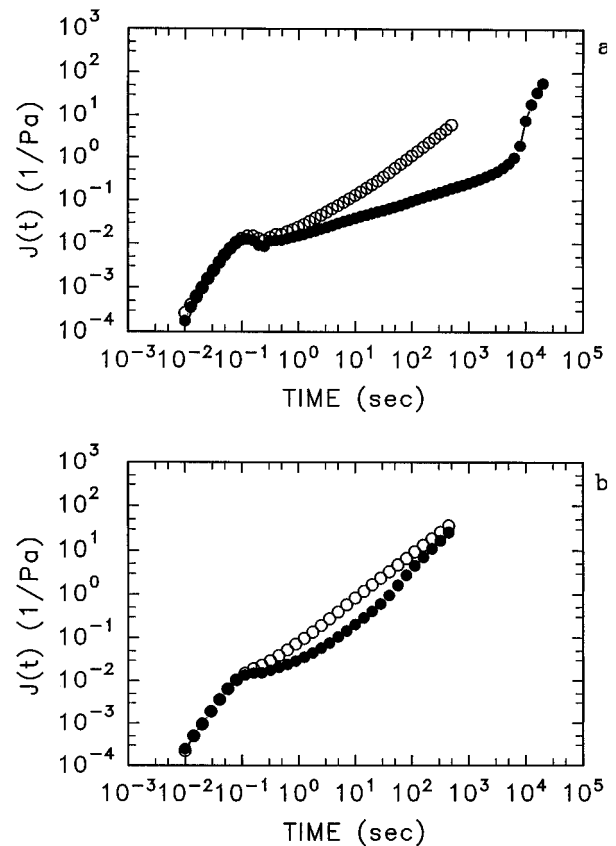


FIG. 2. Typical nonlinear strain response vs time for $\phi^* = 1.03$. (a) $\sigma = 5$ Pa: $\bigcirc$, presheared structure; $\bullet$, pre-fcc structure. (b) $\sigma = 8$ Pa: $\bigcirc$, presheared structure; $\bullet$, pre-fcc structure.

$\simeq 2$ s, the shortest time scale which could be probed, due to instrumental inertia. These results clearly indicate a purely dissipative mechanism as being responsible for the monotonic increase in strain as a function of time, accompanied by viscous restructuring of the suspension as observed via light scattering.
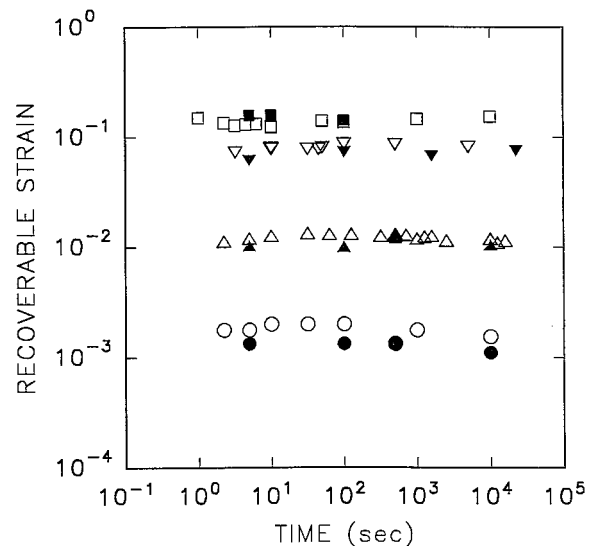


FIG. 3. Typical measured recoverable strain as a function of time. $\phi^* = 1.03$: $\bigcirc$, 0.14 Pa; $\triangle$, 1.0 Pa; $\triangledown$, 5.0 Pa; $\square$, 10.0 Pa. Open symbols represent the initial structure as presheared, and closed symbols as pre-fcc.
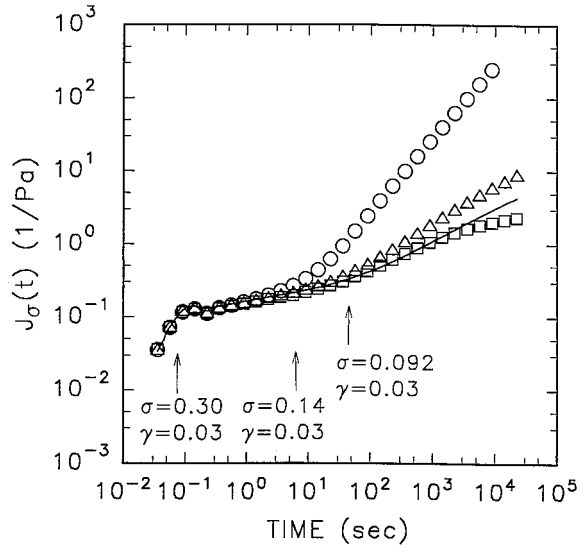
FIG. 4. The creep compliance for presheared structures as a function of stress for the $\phi^* = 0.783$ sample. $\bigcirc$, $\triangle$, and $\square$ represent applied stresses of 0.3, 0.14, and 0.092 Pa, respectively. The solid line represents a pre-fcc structure at a stress of 0.092 Pa. The arrows indicate the point in time where, for each applied stress, the strain reaches 0.03.

Since the microgels exhibit a constant recoverable strain for all applied stresses and over all measurable times, it was expected that linear creep behavior would be found directly from the creep measurements, provided strains were kept below some critical value. Due to the effects of instrumental inertia and the range of stresses examined, small strain behavior obtained with the C14 couette was obscured. However, a limited amount of small strain data was obtained for the $\phi^* = 0.783$ suspension, utilizing a stainless steel double gap couette. Due to its smaller inertial mass and approximately two orders of magnitude decrease in minimum applied stress compared to the C14 cell, the oscillations at small strains were minimized. Although light scattering could not be used to monitor microstructure in this measurement, the same procedure was used which consistently induced presheared and pre-fcc microstructures in the glass couette. These results are shown in Fig. 4, where $\bigcirc$, $\triangle$, and $\square$ represent applied stresses of 0.3, 0.14, and 0.092 Pa, respectively. The solid line represents data obtained for a pre-fcc structure at a stress of 0.092 Pa, and the symbols those of presheared structures. The arrows indicate the point in time where each creep curve reaches a strain of 0.03. As shown, for strains $\leqslant 3\%$; each curve scales on stress (the creep values are identical), indicating linear viscoelastic behavior. Here, the critical strain of 3% is similar to that found in dynamic measurements for this sample, above which we have found nonlinearities in the moduli to appear.

Constant stress dynamic moduli were measured in the linear regime for each induced microstructure, at probing frequencies of $\omega = 0.001-5$ Hz. These results are shown in Figs. 5(a) and 5(b). The lack of frequency dependence of the moduli for $\omega$ below 0.1 Hz indicates that the microgels behave as a viscoelastic solid up to probing times of 1000 s. This is similar to the general behavior of glassy or crystalline polymers, where deformation of the network results in a very broad plateau region, due to hindered mobility of the poly-
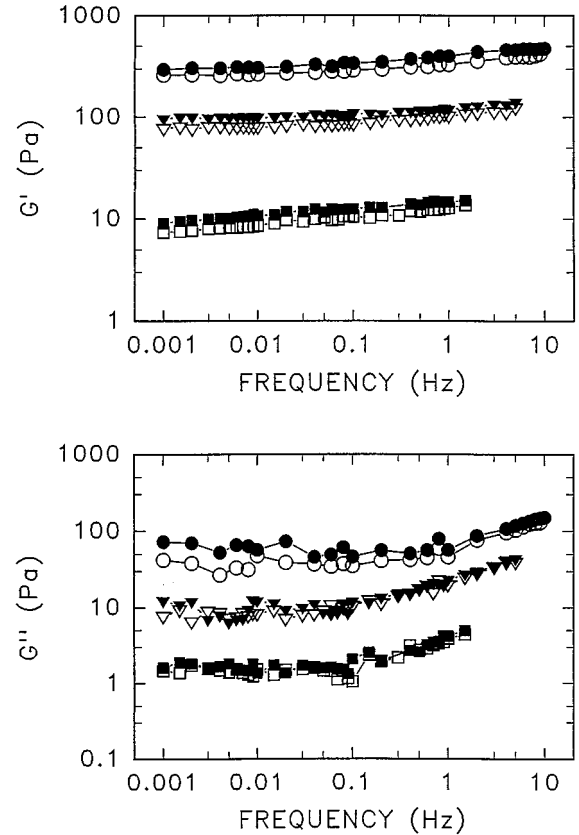


FIG. 5. The (a) storage and (b) loss moduli vs frequency. $\bigcirc$, $\phi^* = 1.218$; $\triangledown$, $\phi^* = 1.03$; $\square$, $\phi^* = 0.783$. The open and closed symbols represent presheared and pre-fcc initial microstructural states, respectively.

mer [14]. Examination of the harmonic content of the measured strain resulted in negligible contributions by frequencies other than the fundamental. As shown, there is a similarity in the moduli as a function of the microstructure. Here, the presheared and pre-fcc microstructures are indicated by open and filled symbols, respectively.

## III. DISCUSSION AND CONCLUSION

We have shown that microstructures in glassy PMMA microgel suspensions, which are geometrically different relative to the direction of flow but are thermodynamically similar, exhibit dramatically different creep behaviors. Although each structure is metastable in these concentrated microgels, the difference in orientation results in vastly different strain behavior for a given applied stress. However, linear dynamic viscoelastic measurements support the essential similarity of microstructure near ''equilibrium,'' while further elucidating the solidlike behavior of these suspensions.

The microstructures found in previous studies of shear-induced states of colloidal suspensions are relevant to the study presented here [4,13]. Real-space geometric structures associated with shear-induced microstructures are depicted schematically in Figs. 6(a) and 6(b). Here the registered stacking of three hexagonal-close-packed (hcp) layers of particles are represented as $A$, $B$, and $C$. If the first layer is $A$, it can be seen from Fig. 6(a) that there are two possible choices for the stacking of the second layer relative to $A$.
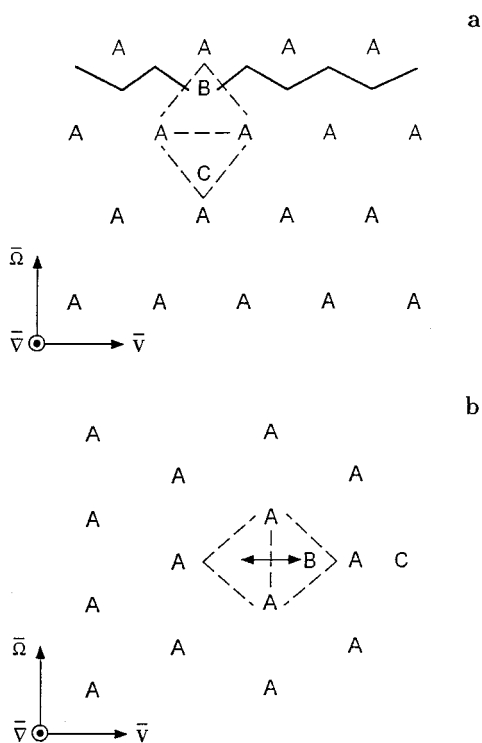
FIG. 6. Stacking of hexagonal-close-packed layers of particles. See text for details.

These are demarcated by the centers of the dashed triangles. Depending upon the crystal structure to be formed, one may specifically place this second layer either in the $B$ position or the $C$ position, or a choice of $B$ or $C$ made at random. If the selection of layer positions relative to the preceding layer are not random, then specific crystal structures may be constructed. Choosing a stacking sequence of $ABAB...$ or $ACAC...$ results in a three-dimensional close-packed structure, while $ABCABC...$ or $ACBACB...$ results in a face-centered-cubic structure. If the position choices are made at random, then a random stacking of layers results. In general, steady and oscillatory shear can result in metastable microstructures which consist of such a random stacking of the hcp layers [4,13]. It is, however, the orientation of the closest-packed direction within these planes, relative to the direction of flow, which has observable rheological consequences in steady shear. The closest-packed direction of Fig. 6(a) is along the direction of flow, while, in Fig. 6(b), it is perpendicular to it. The real space structure of 6a is associated with the scattering shown in Fig. 1(a). This microstructure may easily accommodate an unlimited amount of strain, provided the shear rate is low enough such that the close-packed planes themselves do not become disrupted. Here layers slide past one another while still maintaining registration relative to neighboring layers, following a more or less zigzag line as shown in Fig. 6(a). Thus it would be expected that no large structural evolution would occur during a low but steady applied shear. If the closest-packed direction is aligned along the vorticity direction, the passage of layer $B$ over layer $A$ is limited as shown by the double-headed arrow in Fig. 6(b). A random stacking of hcp planes, with this orientation relative to flow, results in the scattering exhibited in Fig. 1(b). A limited amount of strain ($\sim 1$) will remove

the randomness in layer positions. As all the layers shift to one extreme position, a sequence of $ABCABC...$ or $ACBACB...$ stacking results, which is indicative of a fcc structure. The observed scattering resulting from these fcc twins is shown in Figs. 1(c) and 1(d). Further strain of this structure begins to move the layers beyond the caged region marked by the dashed triangles, eventually disrupting the fcc microstructure. In the scattering, this process is observed as the evolution of microstructure from an fcc structure back into the random stacked hcp alignment of Fig. 1(a). The creep behavior observed in Fig. 2 supports the geometrical considerations above, as the fcc structure exhibits a smaller strain for the same applied stress and measurement time than the structure which allows unlimited and relatively easy slippage of hcp layers. It is simply easier to slide layers past one another as in the structure of Fig. 1(a) than to restructure and eventually reorient the hcp planes in a strained fcc structure. The transition shown in Fig. 2(a) near $10^4$ s is observed to correspond to the reorientation of hcp planes from an $ABCABC...$ stacking sequence to one which is random. At larger applied stresses, this transition is observed to broaden and shift to smaller times.

The recoverable strain is observed to be constant as a function of time and independent of changes in microstructure (see Fig. 3). Furthermore, the creep recovery is the same independent of the applied stress (see Fig. 9). This means that the sample elastic response is the same regardless of the strain deformation of the sample. Such a behavior indicates the elasticity is due to local microstructure and/or particle deformation. The creep recovery relaxation time is less than 2 s in all measurements. Thus the time variation seen in creep measurements (for times greater than the elastic relaxation time) must be due to changes in the viscous dissipation, and caused by changes in the sample microstructure. An immediate consequence is that an instantaneous viscosity $\eta_i$ may be calculated directly from the creep functions

$$\frac{1}{\eta_i(\gamma)} \equiv \frac{dJ_\sigma(t)}{dt}. \tag{1}$$

This instantaneous viscosity is shown for $\phi^* = 1.03$ at $\sigma = 5$ Pa in Fig. 7, along with scattering patterns associated with the viscous response under constant applied stress. The peaked curve, indicated by the filled circles, is the measured instantaneous viscosity versus strain for the pre-fcc structure. The corresponding scattering patterns labeled $A-E$ are associated with the evolution of this structure at the indicated strains. It is observed that this structure evolves from that of random stacked hcp planes, to that of a fcc twin, and finally to a structure similar to the presheared structure. Deformation of the presheared structure is indicated by the open circles, and is observed to be relatively constant, indicating the slippage of layers past one another without catastrophic reorganization of the layers. The scattering pattern for such a structure is identical to that of image $F$, and shows relatively little evolution under the stresses applied, compared to that of the pre-fcc structure. Thus the suspension microstructure is in two different initial states which evolve differently under applied stress, and ultimately end up in the same final microstructural state. This evolution is reflected in the instantaneous viscosity. Here, differences in instantaneous viscos-
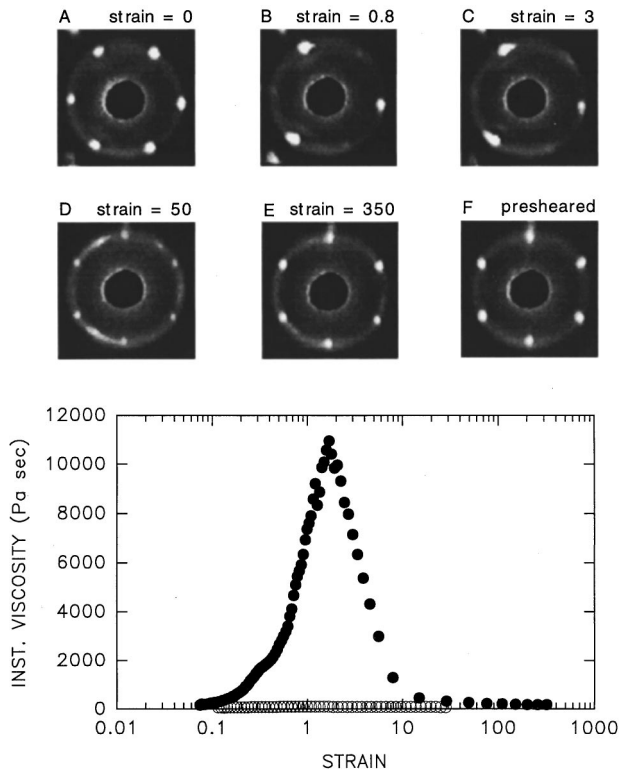
FIG. 7. The instantaneous viscosity as a function of strain for $\phi^* = 1.03$ and $\sigma = 5$ Pa, representing a typical result for samples prepared in a presheared and pre-fcc microstructural state. The observed microstructure is shown by the above scattering images, which correlate with the viscous response, as noted by $A$, $B$, $C$, $D$, and $E$. Image $F$ corresponds to the presheared state. The intensity maxima observed outside the first order scattering ring are also first order scattering maxima but originating from the rear portion of the sample which the laser probe intersects.

ity appear negligible at small strains, but increase dramatically as the strains become large enough to significantly disrupt the structure. The instantaneous viscosities again approach the same value as the microstructures approach similar closest-packed orientations. These results are qualitatively consistent with the earlier geometrical interpretation. In these data, the pre-fcc sample preparation microstructure typically shows a fcc twinning at strains less than 1.0, which is maintained through the peak. As $\eta_i$ starts to decrease, the fcc twin begins to exhibit some distortion, which typically worsens as the strain increases and $\eta_i$ levels off. However, the observed form of $\eta_i$ and strains at which it peaks need to be treated with caution. For a given effective volume fraction, they depend on the applied stress. It is also observed that while the general form of the curve may be the same, a variation in the peak viscosity of up to 30% can occur for repeated runs. The scattering appears the same for these runs, indicating either the lack of sensitivity in the scattering to predict detailed creep behavior or the need for a more careful intensity measurements. The initial rise in $\eta_i$ at a strain of about 0.2 is a common feature for nearly all of our data. This increase in viscosity may be associated with the formation of one of the fcc twins. As expected from the creep curves, measurements of $\eta_i$ at applied stresses larger than that of Fig. 7 typically show a broadening of the peak. Here, the instantaneous viscosity peaks at a lower value as the stress is
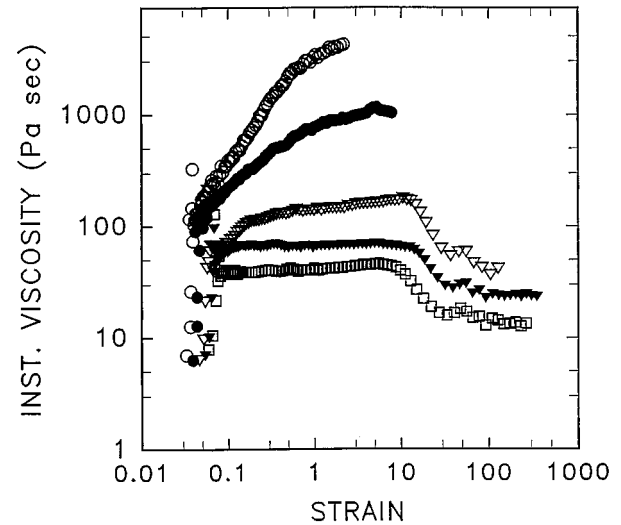


FIG. 8. The instantaneous viscosity as a function of stress and strain for a pre-fcc state, $\phi^* = 0.783$. ($\bigcirc$), $\sigma = 0.3$ Pa. ($\bullet$), $\sigma = 0.35$ Pa. ($\triangledown$), $\sigma = 0.4$ Pa. ($\blacktriangledown$), $\sigma = 0.45$ Pa. ($\square$), $\sigma = 0.5$ Pa.

increased. This is shown in Fig. 8, where $\eta_i$ for the fcc structure is plotted for $\phi^* = 0.783$ at applied shear stresses of 0.3–0.5 Pa. This change in the microstructural and rheological transition behavior with applied stress may at first appear surprising, but these stresses are within the shear thinning regime for steady state viscosity measurements. The stacking model above cannot account for this behavior, as Brownian motion and hydrodynamic and interparticle interactions are not included, and these are needed to understand shear thinning.

Perhaps more surprising are the results shown in Fig. 9. Here, it is observed that the recoverable strain scales on the applied stress. Under deformation, it appears that the suspension elastically stores some of the input energy in a mechanism which responds linearly with stress. The suspension would rather viscously alter its microstructure than elasti-
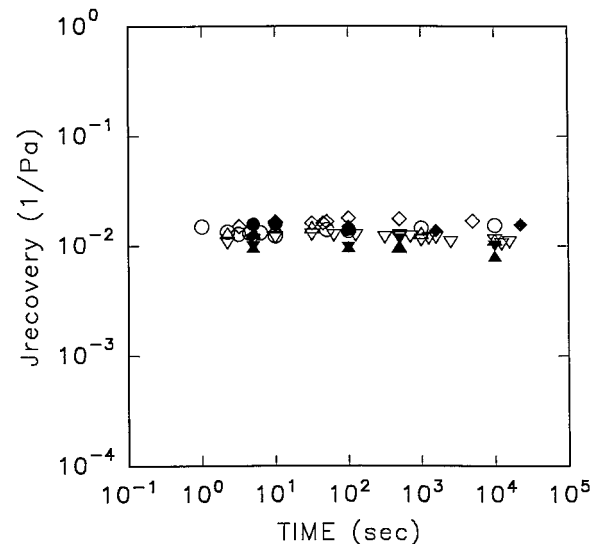


FIG. 9. Recoverable strain shown in Fig. 3 scaled on applied stress. $\phi^* = 1.03$: $\bigcirc$, 0.14 Pa; $\triangle$, 1.0 Pa; $\triangledown$, 5.0 Pa; $\square$, 10.0 Pa. Open symbols represent the initial structure as presheared, and closed symbols as pre-fcc.

cally store energy in a nonlinear way. This recovery behavior could be realized by a mechanism that stores elastic energy in local static particle configurations. Under applied stress, the local configuration would be altered from its metastable state, against the restoring forces due to particle deformation. If the suspension is strained beyond some critical value, the microstructure viscously evolves while keeping the elastic energy stored in the altered configuration constant. This is not contradictory to fact that the applied stresses are in the shear thinning regions, as any stress strain relationship can be considered linear provided the strains are small enough. Here, the strains associated with *particle deformation* may be small enough, and be maintained during restructuring of the suspension under flow. These considerations are corroborated by the observations of Berry, Hager, and Wong in solutions of poly($\alpha$-methylstyrenes) [15]. They found that exceeding a critical stress is a necessary but not sufficient condition to bring about nonlinear viscous flow. A critical strain must also be exceeded, which is suggestive of a viscous microstructural transition with strain, like that observed in our experiments presented here. They defined the following functions to describe nonlinear behavior in creep:

$$\Delta\gamma(t)=\gamma_\eta(t)-\sigma t/\eta_0, \tag{2}$$

$$\gamma_\eta(t)=\sigma J_\sigma(t)-\gamma_{r,\sigma}(t,\infty), \tag{3}$$

where $\gamma_\eta$ represents the viscous contribution to strain due to a nonlinear creep measurement, $\sigma t/\eta_0$ the viscous contribution to strain in the linear limit where $\eta_0$ is the low shear rate plateau viscosity, and $\gamma_{r,\sigma}(t,\infty)$ the measured recoverable strain. It can therefore be seen that $\Delta\gamma(t)$ represents a departure from linearity when greater than zero. Berry, Hager, and Wong found that $\Delta\gamma(t)=0$ for strains up to some critical value, $\gamma_c$, above which $\Delta\gamma(t)$ increases for their materials. This is observed in spite of applied stresses being in the shear thinning region. Below some critical stress, of course, there is no nonlinearity found in the creep behavior, even for strains an order of magnitude larger than $\gamma_c$. In the microgels, the measurement of $J_\sigma(t)$ provides a direct measure of the critical strain because the system is elastically relaxed (for times greater than 2 s). Behavior similar to that found by Berry, Hager, and Wong is found, as shown in Fig. 4. Here, the arrows denote the critical strain of $\gamma_c\sim0.03$ for each stress. The curves scale until the corresponding critical strain is reached. It should be noted that the presheared structure appears to offer a greater resistance to flow than that of the pre-fcc structure contrary to the geometrical interpretation posed earlier. It is unlikely that this is a result of anomalous initial microstructures in these measurements, as this behavior has also been observed at small strains in the $\phi^*=1.22$ sample in the glass couette. Here, the scattering verified the presheared and pre-fcc microstructures. The local hopping from one registration site to another is in the direction of the applied force, and is more direct in the pre-fcc structure, provided it is not pushed too far. The local hopping in the presheared samples is not parallel to the applied force, which implies some reaction force from the sample, and greater resistance to flow. Another possible explanation relies on the role defects play in the presheared structure. The presheared structure generally exhibits a more prominent diffuse Debye-
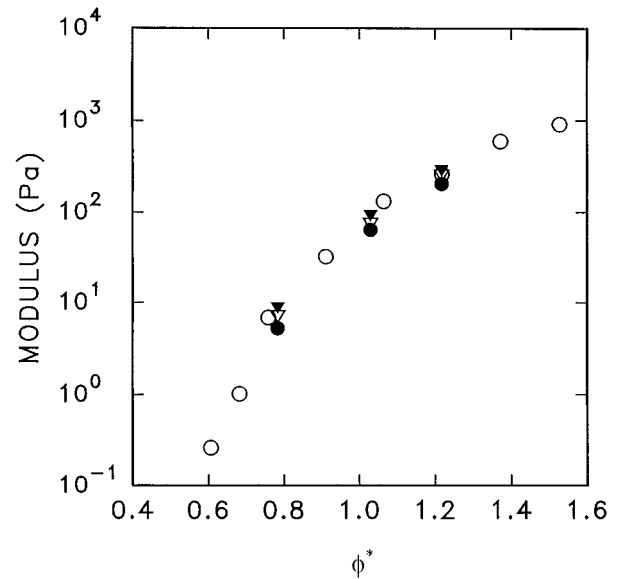


FIG. 10. Measured suspension moduli versus $\phi^*$. $\bigcirc$ and $\triangledown$ represent $G'$ at $\omega=1$ and 0.006 rad/s, respectively. Open and closed triangles represent presheared and pre-fcc microstructures, respectively; $\bullet$, $1/J_{recovery}$ from recovery measurements. Here, presheared and pre-fcc microstructures resulted in nearly identical recoverable compliances. Results for both structures are included in this symbol.

Scherrer ring than the pre-fcc structure, indicating regions of defectlike or liquidlike order existing along with layered structures. It is possible that due to this liquid order, the pre-fcc structure resists flow less than the presheared structure, at small strains greater than the critical strain, but below those producing significant restructuring. Of course, in spite of defects and regions of liquidlike order, the pre-fcc structures exhibit an increased resistance to flow as the microstructure evolves into a full fcc twin.

Since creep and recovery measurements indicate an upper bound of about 2 s for the elastic relaxation time, one expects $G'$ to exhibit the behavior of a viscoelastic liquid, and monotonically decrease with decreasing $\omega$ for $\omega\lesssim0.5$ Hz. Evidence of the elastic nature of the microgels as due to particle deformation lies in this discrepancy between the upper bound relaxation time observed in the creep measurements, and the time scales over which this broad plateau is found in the dynamic moduli. If a mechanism other than particle deformation were responsible for the elastic relaxation, say a configurational relaxation, then this would be reflected in the low frequency response of $G'$ and $G''$. Previous studies of sterically stabilized dispersions of silica hard spheres have observed a high frequency plateau, followed by a roll-off to a slope of 2 when examined over a frequency range of 0.01–100 Hz. This is an indication of a liquidlike response and a single Maxwellian relaxation process [7]. Here the suspensions were not sufficiently concentrated to be glassy, and enough particle mobility was present to allow thermal motion to relax the particle configuration back to equilibrium faster than the rate of perturbation at low frequencies. Increasing volume fractions into the glassy region shifted the observed plateau to lower frequencies, presumably reflecting the increased Brownian relaxation time asso-

ciated with self diffusion. In the microgels, we do not believe the observed plateau to be related to a self diffusive process, but rather to be a result of global structure. The finite loss modulus reflects the dissipative nature of compressively deforming a network of connected microgel spheres under applied stress. In the microgels, the local nature of this deformation can be observed in the similarity of the dynamic moduli as a function of presheared and pre-fcc structures, reflecting the common response of the particles in these two structures in the limit of small strains. When flow is induced under constant applied stress, purely dissipative processes take over, and the suspension behaves as a material with fading memory. Since De is very large given our experimental observation times, the microstructure is "locked" in a metastable state, and diffusive relaxation is negligible. The measured microstructure-dependent instantaneous viscosities are a direct manifestation of this dissipative evolution, with the elastic recovery reflecting the locally deformed particles of the microgel network.

Fitting a straight line to the plot of average total recoverable strain versus stress provides a measure of the recoverable compliance, $J_{recovery}$. A comparison of $1/J_{recovery}$ with the measured value of $G'$ at $\omega = 1$ and 0.006 rad/s is shown in Fig. 10. The $\phi^* = 0.681$ data were incomplete, and $J_{recovery}$ not determined. Although $J_{recovery}$ is typically measured at strains associated with nonlinear behavior and on a time scale shorter than that probed in the dynamic measurements, agreement between the two is observed. We believe

that this is due to the unique compressive nature of the network formed by these microgels, and that $J_{recovery}$ is therefore a measure of the glassy compliance. This is possible given that the measured elastic recovery is local in nature, and not due to global bulk microstructure. This raises an interesting question as to the existence of a true yield stress in these suspensions, although recent measurements on a sensitive Zimm viscometer has not found one.

In summary, the instantaneous viscosity has been determined for a soft sphere suspensions of PMMA spheres swollen in benzyl alcohol. Two separate shear-induced microstructures were examined as a function of strain, and found to exhibit dramatically different behavior. This result was obtainable due to a short elastic relaxation time compared to measurement times, presumably associated with particle deformation. In addition, the storage of elastic energy in these suspensions appears to result from a linear deformation of the particles under applied stress, as the total recoverable strain exhibits scaling on stress. Dynamic measurements of the loss and storage moduli indicate particle deformation in the form of a microgel network, as well as a lack of sensitivity to the microstructures examined.

---

[1] M. Reiner, Phys. Today **17** (1), 62 (1964).

[2] R. B. Bird, O. Hassager, R. C. Armstrong, and C. F. Curtis, *Dynamics of Polymeric Liquids* (Wiley, New York, 1977).

[3] J. C. van der Werff, C. G. de Kruif, C. Blom, and J. Mellema, Phys. Rev. A **39**, 795 (1989).

[4] Bruce J. Ackerson, J. Rheol. **34**, 553 (1990).

[5] S. E. Paulin, Bruce J. Ackerson, and M. S. Wolfe, in *Complex Fluids*, edited by B. Sirota, D. Weitz, T. Witten, and J. Israelachvili, MRS Symposia Proceedings No. 248 (Materials Research Society, Pittsburgh, 1991), p. 259.

[6] S. E. Paulin, Bruce J. Ackerson, and M. S. Wolfe, J. Colloid Interf. Sci. **178**, 251 (1996).

[7] William J. Frith, Trevor A. Stevens, and Jan Mewis, J. Colloid Interf. Sci. **139**, 55 (1990).

[8] Y. D. Yan, J. K. G. Dhont, C. Smits, and H. N. W. Lekkerkerker, Physica A **202**, 68 (1994).

[9] P. N. Pusey and W. van Megen, Nature (London) **320**, 340 (1986).

[10] B. J. Ackerson and P. N. Pusey, Phys. Rev. Lett. **61**, 1033 (1988).

[11] P. N. Pusey, W. van Megen, P. Bartlett, B. J. Ackerson, J. G. Rarity, and S. M. Underwood, Phys. Rev. Lett. **63**, 2753 (1989).

[12] M. S. Wolfe and C. Scopazzi, J. Colloid Interf. Sci. **133**, 265 (1989).

[13] R. L. Hoffman, J. Colloid Interf. Sci. **46**, 491 (1974).

[14] John D. Ferry, *Viscoelastic Properties of Polymers*, 3rd ed. (Wiley, New York, 1980).

[15] G. C. Berry, B. L. Hager, and C.-P. Wong, Macromolecules **10**, 361 (1977).